Modelling the effect of sensory dynamics on a driver's control of a nonlinear vehicle

C. J. Nash & D. J. Cole
Department of Engineering
University of Cambridge, United Kingdom

ABSTRACT: In previous work a linear model of driver steering control was developed which takes account of human sensory dynamics and limitations. In this paper various approaches to modelling a driver's control of a nonlinear vehicle are compared. In contrast to research focussed on modelling the optimal driver, the aim of this work is to develop a realistic model of driver steering behaviour. Simulations were run to compare various nonlinear state estimators and controllers. In general a trade-off was found between simulation time, which could also represent mental load, and controller performance. Experiments are planned to compare the results of these simulations against measured steering behaviour from human drivers.

1 INTRODUCTION

With the growing popularity of active vehicle control systems it is increasingly important to understand how a driver controls a vehicle. Various different approaches have been taken to modelling this control task, with many recent studies following a receding-horizon optimal control scheme (Cole et al. 2006). However, there is a lack of research into how the dynamics and limitations of drivers' sensory systems affect perception and control during driving. A review of the literature showed that control tasks carried out by humans are affected by characteristics of sensory systems such as delays, thresholds and frequency responses (Nash et al. 2016).

In our previous work a new model of driver steering control was developed incorporating models of human sensory dynamics, based on receding-horizon optimal control and assuming optimal integration of multiple noisy sensory measurements. The model was validated using published results from a control task carried out by pilots in a flight simulator (Zaal et al. 2009), and was found to fit these results well (Nash and Cole 2016a). Similar experiments involving a vehicle steering task were designed and carried out by drivers, and an identification procedure was used to find parameter values for the model to fit the results (Nash and Cole 2016b). The model was found to fit the results well, and parameter values were found to be realistic when compared with sensory measurements reported in the literature (Nash et al. 2016).

The new driver model was derived for a linear vehicle, however in more extreme manoeuvres the vehicle may operate near the friction limit of the tyres and the operating point of the vehicle may vary rapidly. It is therefore necessary to develop a model which can describe a driver's control of nonlinear vehicle dynamics. Previous research in this area has generally focussed on modelling the optimal driver, with full state feedback and no sensory dynamics, delays or noise (Ungoren and Peng 2005, Thommyppillai et al. 2009, Keen and Cole 2011). The aim of this work is to find suitable controllers and state estimators for a more realistic nonlinear driver model that takes account of the limitations of a human driver.

2 DRIVER MODEL STRUCTURE

The structure of the new driver model is shown in Figure 1 (Nash and Cole 2016b). Currently it is assumed that the vehicle is travelling at constant speed; longitudinal control will be considered in future work.

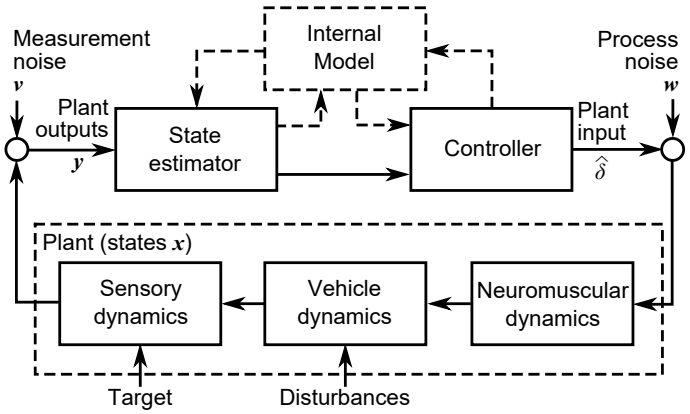

Figure 1: Structure of new driver model

The driver controls a plant which combines the vehicle dynamics with the driver's sensory and neuromuscular dynamics, in order to follow a target path while compensating for disturbances on the vehicle. A state estimator is used to calculate an estimate of the plant states based on the driver's noisy sensory measurements. A controller calculates an optimal plant input $\hat{\delta}$ to minimise a cost function J, weighting the plant input against path-following error e:

$$J = \sum_{k=1}^{\infty} \left(e(k)^2 + q_\delta \hat{\delta}(k)^2 \right) \quad (1)$$

Both the controller and the state estimator make use of an internal model of the plant to predict future trajectories of the plant states. The internal model may not fully match the true system dynamics, with its accuracy likely to be dependent on driver experience (Keen and Cole 2011).

2.1 *Sensory and neuromuscular dynamics*

Previous studies have investigated drivers' neuromuscular dynamics in detail (Pick and Cole 2007), however for simplicity a second-order transfer function is used in this model. Models of the driver's sensory dynamics were chosen based on results from the literature (Nash et al. 2016). The driver's visual system is represented as a measurement of the lateral path-following error plus a 'preview' of the upcoming road path. Models of the driver's vestibular system are also included, using transfer functions to represent the otoliths, which measure acceleration, and semicircular canals, which measure angular velocity. Each of the sensory systems also contains a time delay and sensory noise, arising from the physical properties of the human neurosensory system.

3 NONLINEAR VEHICLE SIMULATIONS

Simulations were run using the driver model to control a nonlinear vehicle. The basic equations of motion for the vehicle were based on the single-track model described in (Nash and Cole 2016b), travelling at a constant speed of 40 m/s. Two different vehicles were simulated, one with understeering characteristics and one with oversteering characteristics.

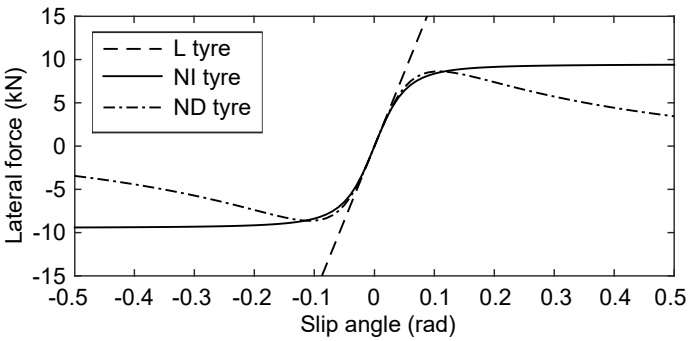

Figure 2: Nonlinear tyre characteristics. Vertical force is 9.5 kN.

Table 1: Nonlinear tyre parameters

Tyre	B	C	D	E
Nonlinear increasing (NI)	12	1.5	1	1
Nonlinear decreasing (ND)	9	2.2	0.909	0.5

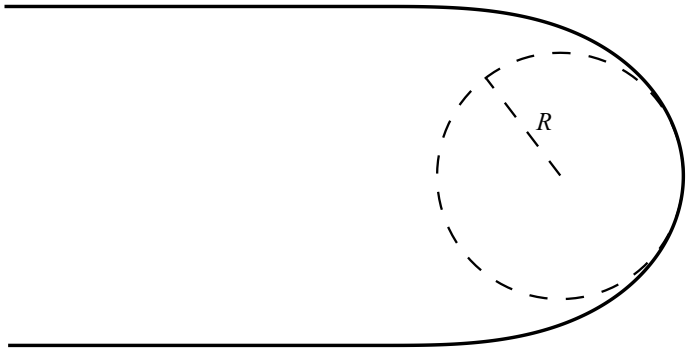

Figure 3: Target path used in simulations

This was achieved by varying the balance of the vertical loads between the front and rear tyres. The loads on the front (F_{zf}) and rear (F_{zr}) tyres were 9.5 kN and 15 kN for the understeering vehicle, and 12kN and 13kN for the oversteering vehicle. Nonlinear tyres were included with lateral characteristics described by the 'magic formula' (Pacejka and Bakker 1992). Three different tyres were simulated: a linear tyre (L), a nonlinear tyre with force monotonically increasing as a function of slip angle (NI), and a nonlinear tyre with force decreasing past the friction limit (ND). The force-slip characteristics of these three tyres are shown in Figure 2, and the nonlinear tyre parameters are given in Table 1. All three tyres have the same cornering stiffness at zero slip angle ($C_f/F_{zf} = C_r/F_{zr} = 18$ rad^{-1}).

The target used for the simulations was a 180° clothoid corner as shown in Figure 3, with the minimum radius R varied to change the operating point of the tyres and the difficulty of the path-following task. Simulations were run with and without measurement and process noise, and also with and without an impulse disturbance added in mid-corner to model a wind gust or bump in the road. Experiments are planned using a driving simulator to test human drivers under similar conditions to these simulations.

4 CONTROLLERS AND STATE ESTIMATORS

Various controllers and state estimators were implemented, varying in their complexity to represent different assumptions about the driver's internal model. Optimal control of a nonlinear plant is a difficult task, which can be simplified through linearisation or transformation of the system dynamics. It is hypothesised that drivers may carry out similar simplifications to reduce their mental load.

The nonlinear plant equations can be written in discrete time state-space form:

$$\boldsymbol{x}(k+1) = f(\boldsymbol{x}(k)) + \mathbf{B}\hat{\delta}(k) + \mathbf{G}\boldsymbol{w}(k)$$

$$\boldsymbol{y}(k) = \mathbf{C}\boldsymbol{x}(k) + \boldsymbol{v}(k) \tag{2}$$

where $\boldsymbol{x}$ is the plant states, $\boldsymbol{y}$ is the plant outputs, $\hat{\delta}$ is the plant input, $\boldsymbol{w}$ is the process noise (including white noise representations of the target and disturbances) and $\boldsymbol{v}$ is the measurement noise. The equations can be linearised about states $\boldsymbol{x}_{\mathrm{L}}$ with the approximation:

$$f(\boldsymbol{x}(k)) \approx \mathbf{A}_{\mathrm{L}}\boldsymbol{x}(k) = \left.\frac{\mathrm{d}f}{\mathrm{d}\boldsymbol{x}}\right|_{\boldsymbol{x}=\boldsymbol{x}_{\mathrm{L}}} \boldsymbol{x}(k) \tag{3}$$

Five different model predictive controllers were implemented, with varying levels of approximation to the nonlinear plant dynamics. These were:

- L0: Linearisation about zero slip angle, $\boldsymbol{x}_{\mathrm{L}} = \mathbf{0}$. A time-invariant controller is derived as for the linear driver model (Nash and Cole 2016b).
- LP0: Linearisation about the initial state $\boldsymbol{x}_0$ of the prediction interval. A new control sequence is calculated at each time step using the MPC derivation presented by Cole et al. (2006), with a constant $\mathbf{A}_{\mathrm{L}}$ linearised about $\boldsymbol{x}_{\mathrm{L}} = \boldsymbol{x}_0$.
- LPF: Linearisation about each state of the prediction interval. The solution starts from a nominal state trajectory $\mathbf{X}_0 = \boldsymbol{x}_0 ... \boldsymbol{x}_{N_p}$, which is the previous optimal sequence shifted by one time step. The linearised matrix $\mathbf{A}_{\mathrm{L}}$ is calculated about each nominal state $\boldsymbol{x}_{\mathrm{L}} = \boldsymbol{x}_n$, and used in an adapted form of the linear MPC derivation in a similar way to Keen and Cole (2011).
- LPF*: LPF constrained to stop the slip angles exceeding 0.107 rad, with a cost on the change in control sequence from the nominal trajectory.
- FNO: Full nonlinear optimisation. The full nonlinear equations are used to predict the plant trajectory over the prediction interval. The Matlab optimisation function *fminunc* is used to find an optimal control sequence at each time step.

Four variations on a Kalman filter were implemented as state estimators and compared with full state feedback. The implementations were all provided by the EKF/UKF Matlab toolbox (Hartikainen et al. 2011), and are based around different approximations to the true nonlinear plant dynamics:

- FSF: Full state feedback: The state estimate is exactly the same as the real states. This removes the effects of sensory dynamics.
- LKF: Linear Kalman filter: A time-invariant Kalman filter is found by linearising the plant states about zero slip angle.
- EKF1: First order extended Kalman filter. A linearised approximation to the plant states is found at each time step.
- EKF2: Second order extended Kalman filter. A quadratic approximation to the plant states is found at each time step.
- UKF: Unscented Kalman filter. The nonlinear plant equations are approximated at each time step using an unscented transform.

5 RESULTS

Two main outcomes of the simulations were analysed: the time taken to run each simulation and the extent to which each combination of controller and state estimator was able to minimise the cost function.

5.1 *Simulation time*

The computational efficiency of each model may be considered as a measure of the mental load on the driver, assuming they are making similar computations. It also affects the practicality of the model for use in engineering applications. The average time taken for simulating each combination of controller and state estimator is shown in Figure 4. There are significant differences between the simulation times, with the times increasing with the accuracy of the approximation to the nonlinear plant. This could reflect the trade-off the driver must make between accuracy and mental load.

5.2 *Controller performance*

The performance of each combination of state estimator and controller can be evaluated by finding the total value of the controller cost function over each simulation. The best performance does not necessarily imply the most realistic, as drivers may carry out sub-optimal control. However this comparison allows the different methods to be compared as a precursor to finding the best fit to experimental results.

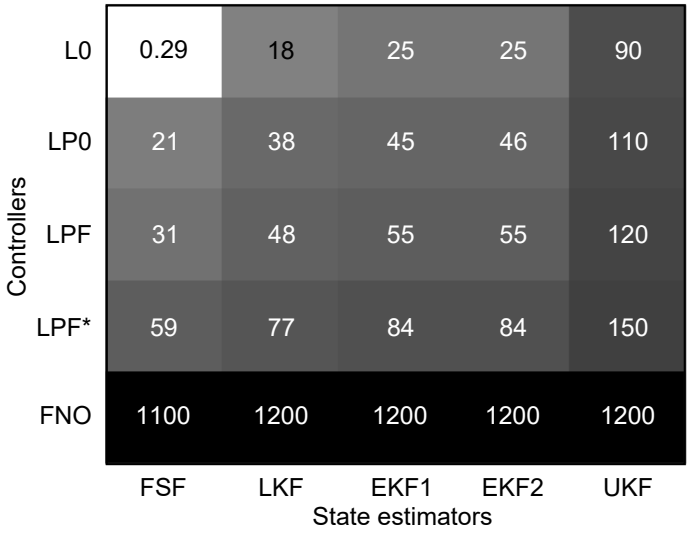

Figure 4: Average time taken (s) for simulation to run using each combination of controller and state estimator.

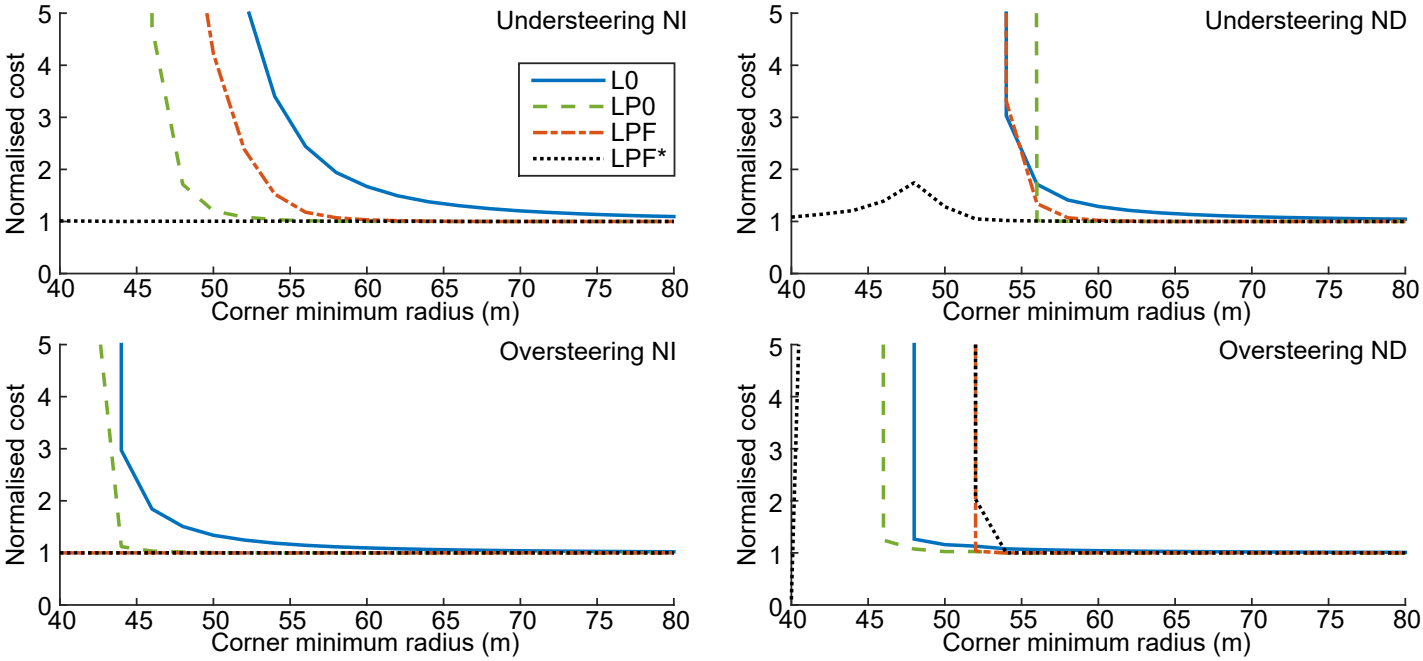

Figure 5: Comparison of the performance of each controller for simulations without added disturbances or noise and with FSF. The total value of the cost function over each simulation has been normalised by the value found for the FNO controller.

The controllers all performed similarly for the linear tyre. A comparison of the different controllers for the nonlinear tyres (with no disturbance or noise) is shown in Figure 5. The cost has been normalised by the cost using the FNO controller. The FNO controller therefore always has a normalised cost of 1, so it can be seen from Figure 5 that FNO was the best performing controller in all cases. For the understeering vehicle with NI tyres the controller performance generally increased with the accuracy of the approximation to the nonlinear dynamics, although LP0 performed better than LPF. However, the modifications carried out for LPF* resulted in a performance as good as FNO. The results for the oversteering NI vehicle are similar, however controller LPF performed as well as LPF* and FNO. This may be because the oversteering vehicle becomes unstable before the tyre force saturates, so the constraints on slip angle are not necessary.

For the ND tyre, the linearised controllers were unable to control the vehicle once the tyre operating point moved beyond the force peak. Adding constraints to prevent this (LPF*) was successful for the understeering vehicle, however LPF* still did not perform as well as FNO for some of the corners. It may be possible to improve the performance of LPF* by tuning the additional cost. For the oversteering vehicle with ND tyres, even controller LPF* was unable to control the vehicle at lower radii, except for the corner with radius 40 m where LPF* outperformed FNO.

The performance of the different controllers with an added disturbance but no noise was qualitatively very similar to the results shown in Figure 5, although with larger overall costs. In some cases controllers LP0 and LPF* performed slightly better than FNO. For a linear plant with white noise disturbances an MPC controller will give an optimal performance, however this is not guaranteed with a nonlinear plant or transient disturbances. Therefore FNO is not guaranteed to be the best controller with disturbances.

5.3 *State estimator performance*

The performance of the state estimators across the different simulations was also compared. In general there was less variation in performance than for the controllers. With no disturbance or noise and with linear tyres, all state estimators performed similarly. For the nonlinear tyres, LKF was not able to give an accurate state estimate, resulting in a higher total cost. However, for the understeering vehicle all the nonlinear state estimators were found to perform similarly, and as well as FSF. The same was seen for the oversteering vehicle with NI tyres, however the performance of the nonlinear state estimators did differ for the oversteering vehicle with ND tyres.

With an added disturbance, the state estimators all performed worse than FSF. This is due to the driver's sensory delays, as the driver is not aware of the disturbance until around 0.2 s after it has occured. In contrast, with FSF the driver has access to all the delay states so is aware of the disturbance straight away, and can react quicker in order to achieve a lower cost. While the state estimators all performed worse than FSF, their performance relative to each other was the same as for the target-only simulations, with the nonlinear state estimators all performing similarly except for the oversteering vehicle with ND tyres.

The performance of the different state estimators for the oversteering vehicle with ND tyres is compared in Figure 6, with and without disturbances. In both cases the state estimators performed as expected for corners with minimum radii greater than around 55 m, where the vehicle starts to become unstable. Below this the state estimates from EKF2 and UKF do

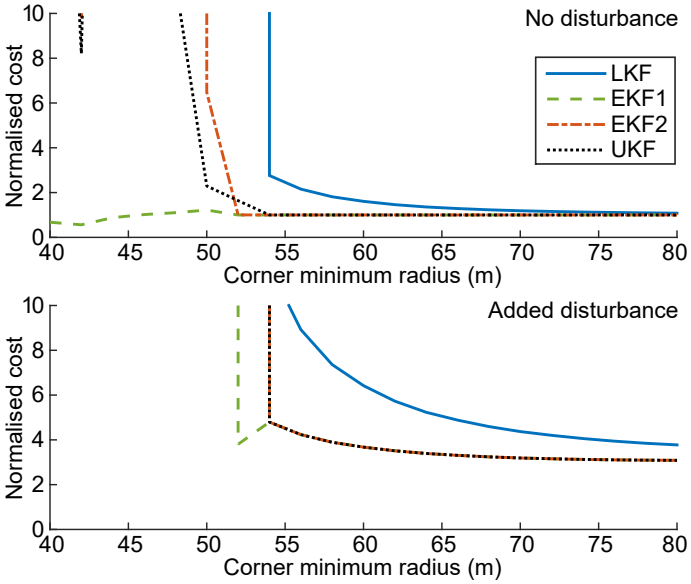

Figure 6: Comparison of the performance of each state estimator for simulations using the oversteering vehicle with ND tyres, no noise and FNO. The total value of the cost function over each simulation has been normalised by the value found with FSF.

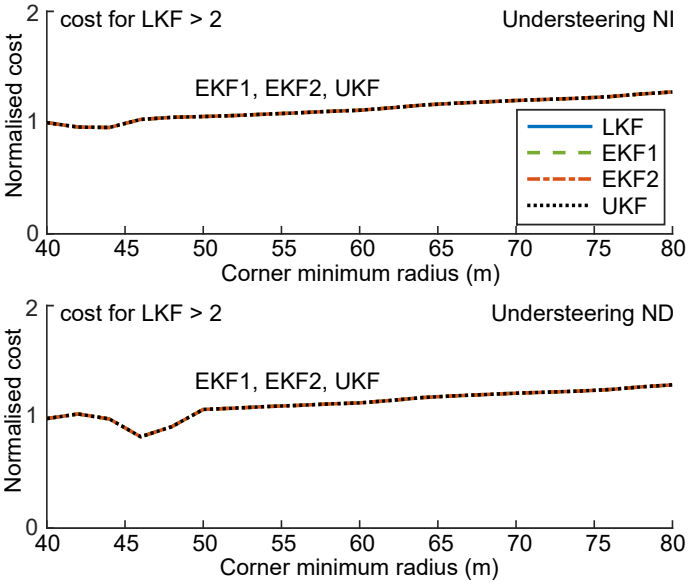

Figure 7: Comparison of the performance of each state estimator for simulations with added noise, using FNO. The total value of the cost function over each simulation has been normalised by the value found with FSF.

not allow the controller to control the vehicle. When there is no disturbance the system can always control the vehicle with EKF1, which even performs better than FSF in some cases. With an added disturbance the system also stops being able to control the vehicle with EKF1, but at a lower radius than EKF2 and UKF.

5.4 *Process and measurement noise*

With added process and measurement noise the performance of the controllers was very similar to the results shown in Figure 5. Similarly to the simulations with a disturbance, for the oversteering vehicle with ND tyres some of the linearised controllers performed better than FNO for some corners. This is because an MPC controller perturbed by white noise isn't guaranteed to perform optimally for a nonlinear plant.

As in the simulations with a disturbance, all linearised Kalman filters performed similarly except for the oversteering vehicle with ND tyres. In general LKF performed worse than these and FSF performed better. However, as shown in Figure 7, in some cases with the understeering vehicle the linearised Kalman filters were better than FSF (with normalised costs less than 1). This may be because the linear Kalman filters effectively smooth the estimated states, reducing potentially suboptimal controller responses to process noise in the nonlinear region of the tyre.

6 DISCUSSION

The results of the simulations can be used to investigate the effect of a driver's sensory dynamics on the control of a nonlinear vehicle. They can also be used to evaluate the controllers and state estimators for use in a driver model, both in terms of how well they model a realistic driver and the practicality of using them in engineering applications. It is also possible to suggest improvements to the controllers which may allow them to run faster or more accurately.

6.1 *Effect of sensory dynamics*

The effect of a driver's sensory dynamics on the control of a nonlinear vehicle can be investigated by comparing the performance of the best state estimator (EKF1) with the results using FSF. Without disturbances or noise the results were the same, showing that for pure target-following the driver's control strategy is not significantly affected by sensory dynamics. However, in real driving there will be disturbances from sources such as wind gusts and road bumps, and driver noise from uncertainties in the driver's sensorimotor system and internal model of the vehicle. With disturbances and/or noise, the cost using EKF1 was generally much higher than with FSF, showing that limitations resulting from the driver's sensory dynamics make it more difficult for the driver to respond to disturbances and noise.

6.2 *Controllers and state estimators*

The results of the simulations showed a large variation in controller performance, and also in time taken to run each controller. In general the performance increased with the time taken, highlighting a trade-off between optimality and complexity. It is possible that the driver makes a similar trade-off in order to reduce their mental load, so the best performing controller may not necessarily be the most realistic. However the driver may use simplifying methods or learned responses to achieve a performance close to optimality without a large 'online' mental load. Experiments are planned using a driving simulator to test how the performance of a real driver compares to the simulations.

LKF was found to perform worse than the other state estimators for nonlinear tyres, as expected. FSF was generally found to perform best with disturbances or noise, however this isn't a good representation of a real driver who is affected by sensory dynamics and delays. In most cases all the nonlinear Kalman filters performed similarly, so it is sensible to choose EKF1 which takes the least time to simulate. For the oversteering vehicle with ND tyres differences were seen between the nonlinear Kalman filters, however EKF1 was found to perform best. Further work is required to understand this driving condition, however it is still possible to get a reasonable overview of driver behaviour while avoiding this specific case.

6.3 *Improvements to controllers*

Various methods can be used to improve the optimality and efficiency of the controllers. It has already been shown that the performance of controller LPF can be improved by adding constraints to limit slip angles, and costs to keep the solution close to the linearised operating point (LPF*). Similar constraints and costs were tested for LP0, however they were found not to be effective. An advantage of FNO over LPF* is that it is able to operate beyond the limit of tyre friction, however it may be possible to develop a combined controller that uses LPF* for smaller slip angles and FNO for larger slip angles.

The practicality of some of the more complex controllers is somewhat limited by the computation time, with each simulation using FNO taking around 10 minutes to complete. There are various approximations which can be made to try and reduce this time, and if done carefully they may not significantly impact the performance of the controller. The simulations were run at a sample frequency of 100 Hz, however driver steering control is unlikely to act over such a high bandwidth. It may therefore be possible to reduce the sample frequency, or maintain a high sampling rate for simulating the plant dynamics while running the controller less frequently. Recent research has investigated intermittent control, where the driver updates their control sequence less frequently and relies on their previous computation in the interval between calculations (Johns and Cole 2015). It may also be possible to calculate some portion of the control strategy offline to reduce the online computational load, which could model drivers' learned behaviours from previous driving experience. Further speed increases may be achieved by writing the algorithms in a compiled language such as C++.

7 CONCLUSION

Simulations have been run to compare various controllers and state estimators for modelling a driver's control of a nonlinear vehicle. In choosing the controller there is generally a trade-off between computation time (mental load) and controller performance. The different nonlinear Kalman filters performed similarly except for an oversteering vehicle with 'nonlinear decreasing' tyres, where a first order extended Kalman filter was found to perform best. Further work is necessary to understand this driving condition. Nonlinear Kalman filters performed as well as full state feedback for pure target-following, showing that the driver's sensory dynamics do not have a significant effect. However with added disturbances or noise the driver's delays and noisy sensory systems resulted in a worse control performance. Experiments are planned to compare the simulations to measured behaviour from human drivers.

8 ACKNOWLEDGEMENTS AND DATA

This work was supported by the UK Engineering and Physical Sciences Research Council (EP/P505445/1, studentship for Nash). Supporting data is available at http://dx.doi.org/10.17863/CAM.595

REFERENCES

Cole, D. J., A. J. Pick, & A. M. C. Odhams (2006). Predictive and linear quadratic methods for potential application to modelling driver steering control. *Vehicle System Dynamics 44*(3), 259–284.

Hartikainen, J., A. Solin, & S. Särkkä (2011). Optimal Filtering with Kalman Filters and Smoothers - a Manual for the Matlab toolbox EKF/UKF.

Johns, T. A. & D. J. Cole (2015). Measurement and mathematical model of a driver's intermittent compensatory steering control. *Vehicle System Dynamics 53*(12), 1811–1829.

Keen, S. D. & D. J. Cole (2011). Application of time-variant predictive control to modelling driver steering skill. *Vehicle System Dynamics 49*(4), 527–559.

Nash, C. & D. Cole (2016a). Development of a novel model of driver-vehicle steering control incorporating sensory dynamics. In M. Rosenberger, M. Plöchl, K. Six, and J. Edelmann (Eds.), *The Dynamics of Vehicles on Roads and Tracks*, pp. 57–66. Graz, Austria: CRC Press.

Nash, C. J. & D. J. Cole (2016b). Identification of a novel model of driver steering control incorporating human sensory dynamics. *Manuscript submitted for publication*.

Nash, C. J., D. J. Cole, & R. S. Bigler (2016). A review of human sensory dynamics for application to models of driver steering and speed control. *Biological Cybernetics 110*(2-3), 91–116.

Pacejka, H. B. & E. Bakker (1992). The magic formula tyre model. *Vehicle System Dynamics 21*(S1), 1–18.

Pick, A. J. & D. J. Cole (2007). Dynamic properties of a driver's arms holding a steering wheel. *Proceedings of the Institution of Mechanical Engineers, Part D: Journal of Automobile Engineering 221*(12), 1475–1486.

Thommyppillai, M., S. Evangelou, & R. S. Sharp (2009). Car driving at the limit by adaptive linear optimal preview control. *Vehicle System Dynamics 47*(12), 1535–1550.

Ungoren, A. & H. Peng (2005). An adaptive lateral preview driver model. *Vehicle System Dynamics 43*(4), 245–259.

Zaal, P. M. T., D. M. Pool, M. Mulder, & M. M. van Paassen (2009). Multimodal Pilot Control Behavior in Combined Target-Following Disturbance-Rejection Tasks. *Journal of Guidance, Control, and Dynamics 32*(5), 1418–1428.